

Consumption of *S*-Allylcysteine Inhibits the Growth of Human Non-Small-Cell Lung Carcinoma in a Mouse Xenograft Model

FENG-YAO TANG,^{*,†,||} EN-PEI CHIANG,^{§,||} AND MAN-HUI PAI[#]

[†]Biomedical Science Laboratory, Department of Nutrition, China Medical University, 40402 Taichung, Taiwan, [§]Department of Food Science and Applied Biotechnology, National Chung-Hsing University, Taichung, Taiwan, and [#]Department of Anatomy, Taipei Medical University, 11031 Taipei, Taiwan.

^{||}These authors equally contributed to this work.

Lung cancer is one of the leading causes of cancer death in the world. Human non-small-cell lung carcinoma (NSCLC) accounts for almost 80% of lung cancer cases. Aberrant phosphoinositide 3-kinase (PI3K)/Akt/mTOR signaling pathways play important roles and have been widely observed in the development of NSCLC. Previous studies indicated that garlic extracts such as diallyl disulfide (DADS) and diallyl trisulfide (DATS) could inhibit the proliferation of several types of cancer in vitro. However, the inhibitory effects of *S*-allylcysteine (SAC) on the growth of NSCLC have not been demonstrated yet. Therefore, this study investigated whether consumption of SAC could prevent the growth of NSCLC in both in vitro and in vivo models. It was found that SAC significantly inhibited the proliferation of human NSCLC A-549 cells in vitro. Treatment of the NF- κ B inhibitor, Bay-11-7082, could significantly inhibit the proliferation of NSCLC A-549 cells. The results demonstrated that SAC significantly suppressed the activation of mTOR, NF- κ B, and cyclin D1 molecules in vitro. Furthermore, the results demonstrated that consumption of SAC significantly inhibited the growth of highly metastatic human NSCLC cells in tumor-bearing mice. Bioluminescence imaging and pathological and immunohistochemical (IHC) staining results also indicated that SAC could effectively suppress the growth and malignant progression of human NSCLC in vivo. The chemopreventive effects of SAC were associated with suppression of mTOR and NF- κ B molecules in vivo. These results suggested that SAC could act as an effective agent against the malignant progression of human NSCLC in both in vitro and in vivo models.

KEYWORDS: *S*-Allylcysteine; mTOR; NF- κ B; proliferation; bioluminescence imaging; human non-small-cell lung cancer

INTRODUCTION

Lung cancer is the leading cause of malignancy-related death in the Western world (1, 2). Clinically, lung cancer is classified into two categories: non-small-cell lung carcinoma (NSCLC) and small-cell lung carcinoma (SCLC). NSCLC accounts for approximately 85% of carcinoma cases, and SCLC constitutes almost all of the remaining ones. Somatic mutation of multiple proto-oncogenes and tumor suppressor genes would lead to the tumorigenesis of lung cancer. Generally, cancer development results from aberrant cell proliferation and abnormalities in apoptosis. Several molecular targets responsible for cancer development have been extensively studied in the past few years. The phosphoinositide 3-kinase (PI3K)/Akt signaling pathway has been shown to be the predominant growth-factor-activated pathway in the tumorigenesis of many types of cancer (3–6). The downstream mammalian target of rapamycin (mTOR) has been further identified as a target of the PI3K/Akt signaling pathway (7). The PI3K/Akt/mTOR signaling pathway controls the cell cycle progression and cell proliferation of

NSCLC (8, 9). The amplification of these signaling pathways could lead to aberrant proliferation of cancer cells and tumorigenesis. During the activation of these signaling pathways, cell cycle related proteins such as cyclin D1 and proliferating cell nuclear antigen (PCNA) are major regulators for cell-cycle progression and DNA replication, respectively (10, 11). A recent study indicated that p21^{CIP1/WAF1} protein may serve as a cell-cycle inhibitor protein and suppress the functions of cyclin D1 and PCNA proteins (10, 11). The activated Akt/mTOR signaling pathway has been found in NSCLC and uncovered essential roles in the control of gene expression and protein translation, which affect cellular proliferation and tumor angiogenesis. Previous studies indicated that PI3K-dependent phosphorylation of Akt or mTOR molecules in a panel of NSCLC cell lines was correlated with resistance to chemotherapy (3). The mTOR inhibitor rapamycin alone or in combination with chemotherapy treatment rendered NSCLC cell lines with highly Akt/mTOR more responsive to apoptosis and growth inhibition (7, 12). Collectively, these pieces of evidence show significant roles of the activated EGFR and PI3K/Akt/mTOR pathway in NSCLC. Previous study indicated that the PI3K signaling pathway modulates cellular progression of NSCLC (13). The activated Akt signaling pathway is also involved in the expression of cyclooxygenase-2 (COX-2) of many types of cancer cells. Regulation of

*Address correspondence to this author at the Biomedical Science Laboratory, Department of Nutrition, China Medical University, 91 Hsueh-Shih Rd., 40402 Taichung, Taiwan (phone (886-4) 22060643; fax (886-4) 22062891; e-mail vincenttang@mail.cmu.edu.tw).

COX-2 gene expression is mainly regulated by several transcription factors such as nuclear factor- κ B (NF- κ B) through the PI3K/Akt signaling pathway (14). The active NF- κ B consists of a dimer of a REL family protein (p65) and a p50 or p52 subunit. NF- κ B is maintained in the cytoplasm through interaction with inhibitors of NF- κ B (I κ B) (14). Upon stimulation, NF- κ B is translocated into the nucleus and promotes cancer cell proliferation, invasion, and malignancy. Suppression of the Akt/NF- κ B signaling pathway could lead to the suppression of cellular proliferation and malignancy (14–16). Small molecules that target the Akt/mTOR pathway may effectively cure lung cancer. Therefore, the regulation of the PI3K/Akt/NF- κ B signaling pathway and COX-2 may become possible targets for anticancer drug treatment or nutritional intervention.

Current treatments for lung cancer patients include surgery, radiotherapy, and chemotherapy. Although chemotherapy could improve the 5-year survival rate of NSCLC patients up to 15%, the lack of effective approaches is still widespread. Experimental data demonstrate that the active ingredients in garlic (*Allium sativum*) extracts including S-allylcysteine (SAC), diallyl disulfide (DADS), and diallyl trisulfide (DATS) have anticarcinogenic effects and inhibit the growth of several types of cancer (17–21). Epidemiological studies suggested that consumption of garlic might have protective effects against several types of cancer including stomach and colon (22, 23). However, to date, the in vitro and in vivo inhibitory effects of SAC on the proliferation of human lung cancer cells have not been demonstrated. Therefore, in this study, we determined the molecular actions of SAC on malignant progression of human NSCLC A-549 cells in both in vitro cell culture and in vivo mouse xenograft models.

MATERIALS AND METHODS

Reagents and Antibodies. S-Allylcysteine with purity of >98% was purchased from LKT Laboratories, Inc. (St. Paul, MN). Anti-PCNA, anti-NF- κ B, antiphosphorylation Akt, and antiphosphorylation mTOR monoclonal antibodies were purchased from Cell Signaling Technology, Inc. (Danvers, MA). Anti- β -actin antibody was purchased from Sigma (St. Louis, MO). Human NSCLC A-549 cell line with luciferase reporter gene was purchased from Caliper Life Sciences Inc. (Hopkinton, MA). RPMI-1640 medium and phosphate-buffered saline (PBS) were purchased from Invitrogen Inc. (Carlsbad, CA). Tissue lysis kit was purchased from Pierce Biotechnology Inc. (Rockford, IL). S-Allylcysteine was dissolved in distilled water at a concentration of 400 mM and stored at -20°C . Immediately before the experiment, different concentrations of SAC solution were freshly prepared and given to NSCLC A-549 cancer cells or experimental animals.

Cell Culture. Briefly, human NSCLC A-549 cells were cultured in a 37 $^{\circ}\text{C}$ humidified incubator with 5% CO_2 and grown to confluency using fetal bovine serum (FBS) supplemented RPMI-1640 media. Cells used in different experiments have a similar passage number. RPMI-1640 medium was supplemented with 10% heat-inactivated FBS, 2 mM L-glutamine, and 1.5 g/L sodium bicarbonate in the absence of antibiotics.

Assessment of Cell Proliferation. The MTT assay was conducted to detect cell proliferation. Human NSCLC A-549 cells were seeded in 24-well plates, each well containing 1×10^5 cells. After 24 h, the culture medium was replaced by medium with SAC or specific inhibitors for different signaling pathways. There were triplicates for each concentration. At different time points, the 24-well plate was taken out and fresh 3-[4,5-dimethylthiazol-2-yl]-2,5-diphenyltetrazolium bromide (MTT, final concentration of 0.5 mg/mL in PBS) was added to each well. After 2 h of incubation, the culture media were discarded, 200 μL of acidic isopropanol was added to each well, and the plate was vibrated to dissolve the depositor. The optical density was measured at 570 nm with a microplate reader.

Xenograft Implantation of Tumor Cells. Briefly, human NSCLC A-549 cells were maintained at 37 $^{\circ}\text{C}$ in a 5% CO_2 incubator and grown to confluency using 10% FBS and 0.15% (w/v) sodium bicarbonate RPMI-supplemented media. To produce a mouse xenograft model, subconfluent cultures of NSCLC A-549 cells were given fresh medium 24 h before being

harvested by a brief treatment with 0.25% trypsin and 0.02% EDTA. Trypsinization was stopped with medium containing 10% FBS, and the cells were washed twice and resuspended in serum-free medium. Only single-cell suspensions with a viability of >90% were used for injections.

Animals, Diet, and SAC Supplementation. Adult (3–4 weeks old) BALB/CAnN-Foxn1 nude mice (22–25 g) were obtained from the National Laboratory Animal Center (Taipei, Taiwan). Mice were maintained under specific pathogen-free conditions in facilities approved by the National Laboratory Animal Center in accordance with current regulations and standards (animal protocol no. 97-5-D). During the entire experimental period, mice were fed a standard Lab 5010 diet purchased from LabDiet Inc. (St. Louis, MO). The standard diet contains crude fat (13.5% total energy of diet), protein (27.5% total energy of diet), and carbohydrate (59% total energy of diet) and had no detectable amounts of SAC as indicated by the supplier.

Mice anesthetized with an inhalation of isoflurane were placed in a supine position. Human NSCLC A-549 cells ($1 \times 10^6/0.1$ mL medium) were inoculated into BALB/C nude mice. A well-localized bleb was a sign of a technically satisfactory injection. After the inoculation, mice were divided into three subgroups. SAC was dissolved in distilled water and given to nude mice by gavage once a day at a total volume 0.15 mL. One group (low dosage of SAC) received daily oral consumption of SAC dissolved in distilled water at a dose of 240 mg/kg of body weight (BW) once per day. The other group (high dosage of SAC) received daily oral consumption of SAC at a dose of 480 mg/kg of BW once per day. The tumor control group received only distilled water. Body weights were also measured once weekly. Following 8 weeks of treatment, the mice were sacrificed, and tissues including tumors were frozen immediately, sectioned, and stained with hematoxylin–eosine (H&E) for light microscopic analysis.

Bioluminescence Imaging of Tumor. Documentation of bioluminescence imaging was performed by using an in vivo imaging system (IVIS). Luciferin (15 mg/mL), the substrate of luciferase, was injected into the tumor-bearing mice peritonally. Results of bioluminescence imaging were analyzed by accessory software. The average bioluminescence intensity was correlated to the size of tumor tissue and presented as proliferation index.

Pathological and Immunohistochemical Stainings of Tumor Tissues. Frozen tumor tissues were cut in 5 μm sections and fixed immediately. Sections were stained with Mayer's H&E. Negative controls did not show staining. In a blinded manner, several hot spots were examined per tumor section (high-power fields $\times 200$) in each group. Images of tumor sections were acquired on an Olympus BX-51 microscope using the Olympus DP-71 digital camera and imaging system.

Preparation of Protein Extraction. Cell lysates from animal tissues were prepared using a Tissue Extract reagent kit containing protease inhibitor and phosphatase inhibitors according to the manufacturer's instruction. After centrifugation for 10 min at 12000g to remove cell debris, the supernatants were retained as a whole tissue extract. Cross-contamination between nuclear and cytoplasmic fractions was not found (data not shown).

Western Blotting Analysis. Briefly, tissue proteins or cell lysates were extracted according to the manufacturer's instruction. Cellular proteins (100 μg) were fractionated on 10% SDS-PAGE, transferred to nitrocellulose membrane, and blotted with anti-NF- κ B p65 (Rel A) monoclonal antibody, according to the manufacturer's instructions. The blots were stripped and reprobed with either β -actin or lamin A/C antibodies as loading control. Levels of phosphorylated mTOR, cyclin D1, p21^{CIP1/WAF1}, PCNA, and phosphorylation Akt in cell lysates or tumor tissues were measured by using the same procedure described above.

Statistical Analysis. The quantitative methodology was used to determine whether the difference in the tumor weight or proliferation index among experimental sets Low_SAC, High_SAC, and tumor control sets ($n = 6$ for each group) in human NSCLC cancer cells bearing mice. In brief, statistical analyses of the differences in tumor weight or proliferation index among experimental and control conditions were performed using SYSTAT software. Confirmation of difference in tumor weight or proliferation index as being statistically significant requires rejection of the null hypothesis of no difference between mean weight obtained from duplicate sets of experimental and control groups at the $p = 0.05$ level with the one-way ANOVA model. The Bonferroni post hoc test was used to determine differences among different groups.

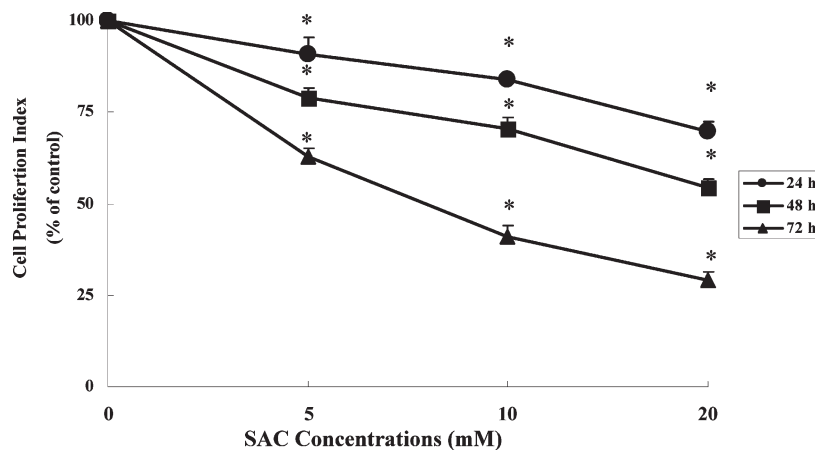


Figure 1. Inhibitory effects of SAC on the proliferation of human NSCLC A-549 cells in vitro. Human lung cancer cells, cultured in RPMI-1640 medium with 10% FBS in a tissue culture dish, were lifted off by trypsinization, pelleted by centrifugation, and resuspended in the same medium. Approximately 100,000 cells were seeded on each well of a 24-well plate. The human lung cancer cells were then cultured in RPMI-1640 medium with SAC (0, 5, 10, and 20 mM) for 24, 48, and 72 h until measurement of cell proliferation. The incubation was stopped at different time points and measured with MTT assays for cell proliferation. The analysis of cell proliferation was described under Materials and Methods. Data from three separate experiments are shown as the mean \pm SEM. Similar results were observed from two independent experiments. Asterisks represent statistically significant difference compared to the control group, $p < 0.05$. The data shown are representative of three independent experiments.

RESULTS

Inhibitory Effects of SAC on the Proliferation of Human NSCLC A-549 cells in Vitro. As shown in **Figure 1**, SAC significantly inhibited cell proliferation of human NSCLC A-549 cells in vitro. At 24 h, SAC (at concentrations of 5, 10, and 20 mM) effectively suppressed the proliferation of human NSCLC A-549 cells up to 10, 17, and 30%, respectively. At 48 h, SAC (at concentrations of 5, 10, and 20 mM) significantly suppressed the proliferation of human NSCLC A-549 cells up to 22, 30, and 46%, respectively. Furthermore, SAC could significantly suppress the proliferation of human NSCLC A-549 cells up to 37, 59, and 71% at 72 h, respectively. This also implied that SAC even at a low concentration of 5 mM could still effectively inhibit the proliferation of human NSCLC A-549 cancer cells at 72 h. These results suggested that SAC with chemopreventive effects could significantly suppress the proliferation of human lung cancer A-549 cells in dose-dependent and time-dependent manners.

SAC Modulated Akt/mTOR/NF- κ B Signaling Pathways in Human NSCLC A-549 Cells. To further examine the possible signaling pathways involved in the regulation of cell proliferation, we treated human NSCLC A-549 cells with specific inhibitors for different signaling pathways. As shown in **Figure 2A**, our results indicated that treatment of wortmannin (a specific inhibitor of PI3K) and Bay-11-7082 (a specific inhibitor of NF- κ B) significantly suppressed cellular proliferation of human NSCLC A-549 cells at 24 and 48 h, respectively. However, PD098059 (a specific inhibitor of MEK) could mildly inhibit the survival of human A-549 cells. These results suggested that PI3K/Akt/NF- κ B signaling pathways played important roles in the regulation of cellular proliferation of human NSCLC A-549 cells.

To examine the possible actions of SAC in NSCLC A-549 cells, we measure the effects of SAC on the downstream molecules of PI3K signaling pathway. As shown in **Figure 2B**, SAC (at a concentration of 20 mM) could time-dependently inhibit the activation of p-mTOR and NF- κ B p65 (Rel A) molecules without any change of actin protein. The quantitative results and statistical analysis of these proteins are shown in **Figure 2C**. Thus, it is plausible that SAC could modulate the cell proliferation in part through suppression of the PI-3K/Akt/mTOR signaling pathway and NF- κ B molecule.

SAC Modulated the Expression of Cyclin D1 Proteins in Human NSCLC A-549 Cells. Due to the inhibitory effects of SAC on the proliferation of human NSCLC A-549 cells, we further investigated the possible actions of SAC on the expression of cell-cycle modulator proteins such as cyclin D1 proteins. As shown in **Figure 3A**, our results demonstrated that SAC significantly inhibited the expression of cyclin D1 proteins in a time-dependent manner. Because cell-cycle inhibitory protein p21^{CIP1/WAF1} plays an important role in the regulation of cycle cell, we further investigated the effects of SAC on the expression of p21 protein. As shown in **Figure 3A**, SAC could significantly induce the expression of p21 protein. The quantitative results and statistical analysis of these proteins are shown in **Figure 3B**. Taken together, our results indicated that SAC could suppress cell proliferation in part through the modulation of cell-cycle regulatory proteins.

Consumption of SAC Suppressed the Growth of Lung Carcinoma in Vivo. To further prove our hypothesis, we investigated the inhibitory effects of SAC on the growth of human lung carcinoma in vivo. We adapted a mouse xenograft model by inoculating human NSCLC A-549 cells with luciferase reporter gene into nude mice. We evaluated the in vivo inhibitory effects of SAC on highly metastatic neoplasm by using a bioluminescence imaging (BLI) system. To demonstrate the growth rate of lung cancer in vivo, we measured the bioluminescence intensity emitted from A-549 cells once a week. As shown in **Figure 4A**, consumption of SAC could significantly inhibit the tumor growth rate at dosages of 240 and 480 mg/kg of BW. Furthermore, dietary intake of SAC (240 and 480 mg/kg of BW/day) could effectively reduce the in vivo bioluminescence intensity represented as proliferation index after 8 weeks of experiment period (**Figure 4B**). In comparison to the control group (no SAC treatment), consumption of SAC (at a daily dosage of 240 or 480 mg/kg of BW) significantly reduced tumor weight 0.42- and 0.64-fold, respectively ($n = 6$) (**Figure 4C,D**). Taken together, it is probable that consumption of SAC could act as an effective chemopreventive agent and significantly suppress the in vivo growth of NSCLC A-549 cells in a mouse xenograft model.

Inhibitory Effects of SAC on Cellular Proliferation Are Associated with the Reduced Expression of PCNA Protein in NSCLC A-549 Cell Transplanted Nude Mice. To further identify the inhibitory effects of SAC on tumor malignancy, we documented the

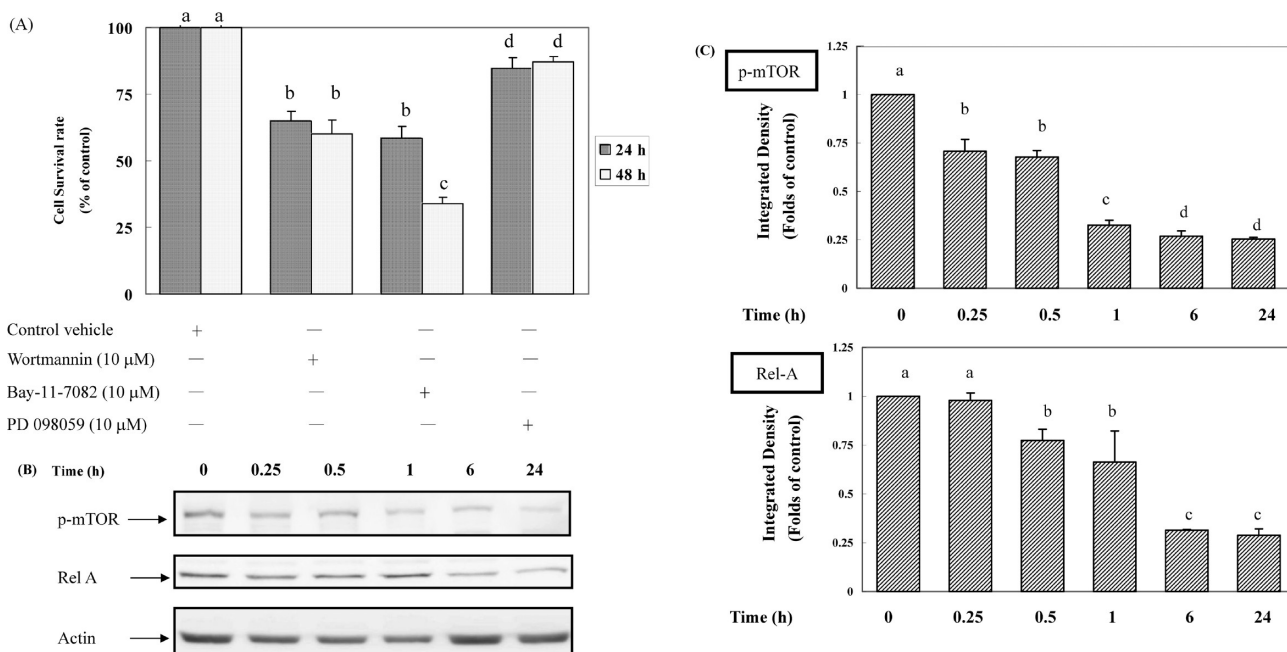


Figure 2. SAC modulated Akt/mTOR/NF- κ B signaling pathways in human NSCLC A-549 cells. **(A)** Postconfluent lung cancer cells cultured on 24-well plates were incubated in RPMI-1640 medium with 10% fetal bovine serum at 37 °C. After washing out the media, lung cancer cells were incubated with DMSO (control vehicle), wortmannin, Bay-11-7082, and PD 098059 at 37 °C for different time points (24 and 48 h) until measurement of cell proliferation. The incubation was stopped at different time points and measured with MTT assays for cell proliferation. The analysis of cell proliferation was described under Materials and Methods. Data from three separate experiments are shown as the mean \pm SEM. Similar results were observed from two independent experiments. Different letters represent statistically significant difference, $p < 0.05$. The data shown are representative of three independent experiments. **(B)** Postconfluent lung cancer cells cultured on 10 cm culture dishes were incubated in RPMI-1640 medium with 10% fetal bovine serum at 37 °C. After washing out the media, lung cancer cells were incubated with SAC (20 mM) for different time points. Cell lysates from A-549 cells were prepared using a NE-PER reagent kit containing protease inhibitor and phosphatase inhibitors according to the manufacturer's instruction. After centrifugation for 10 min at 12000g to remove cell debris, the supernatants were retained as a cytoplasmic extract. Cell lysates were blotted with antiphosphorylation mTOR and anti-NF- κ B p65 (Rel A) monoclonal antibodies as described under Materials and Methods. The levels of detection in cell lysate represent the amount of phosphorylated mTOR and Rel A proteins in human lung cancer A-549 cells. The blots were stripped and reprobed with anti-actin antibody as loading control. The results presented are representative of three different experiments. The immunoreactive bands are noted with arrows. **(C)** The integrated density of p-mTOR and Rel A proteins adjusted with internal control protein (actin) are shown. Different letters represent statistically significant difference, $p < 0.05$.

pathological changes through Mayer's H&E staining or immunohistochemical staining of tumor tissues. As shown in **Figure 5A-1**, H&E staining results showed high levels of proliferating cells (irregular nuclei stained with blue color) in tumor tissues. However, consumption of either low dosage (240 mg/kg/day) or high dosage (480 mg/kg/day) of SAC had lower levels of proliferating cells (**Figure 5A-2,A-3**). These results suggested that consumption of SAC could significantly suppress the proliferation of cancer cells and inhibit the malignancy of lung carcinoma.

To investigate whether SAC could inhibit tumor growth in vivo, we further analyzed the nuclear expression of PCNA protein in experimental animals. As shown in **Figure 5B**, consumption of SAC could significantly suppress the accumulation of nuclear PCNA protein in tumor-bearing mice. The quantitative results and statistical analysis of PCNA protein are shown in the bottom panel. In **Figure 5C**, immunohistochemical staining results also demonstrated consumption of SAC could reduce the level of PCNA-positively stained NSCLC cells. Quantitative results also showed that SAC could significantly reduce the PCNA expression level from the results of immunohistochemical staining. These results demonstrated that consumption of SAC could effectively reduce PCNA expression and suppress the growth of human lung carcinoma in tumor-bearing mice.

Consumption of SAC Suppressed the Malignant Progression of Lung Carcinoma and Modulated the Expression of NF- κ B and COX-2 Proteins in Tumor-Bearing Mice. To identify the possible mechanisms of action, we investigated the inhibitory effects of SAC on PI3K/Akt signaling pathway. As shown in **Figure 6A**,

increased levels of phosphorylated Akt, mTOR, and activated NF- κ B proteins were widely observed in tumor tissues. However, consumption of SAC at different dosages (240 and 480 mg/kg of BW) could significantly suppress the activation of the Akt/mTOR signaling pathways and the activation of NF- κ B p65 (Rel A) proteins in a NSCLC mouse xenograft model. Quantitative results also showed that consumption of SAC at different dosages (240 and 480 mg/kg of BW) could effectively reduce the phosphorylation of mTOR protein and expression NF- κ B p65 (Rel A) proteins to <25% of control group (tumor-bearing group). To further investigate the inhibitory effects of SAC on malignant progression of lung carcinoma, we measured the levels of COX-2 positively stained cells by using immunohistochemical staining. As shown in the **Figure 6B**, mice inoculated with NSCLC A-549 cells had increased levels of COX-2 protein. Furthermore, consumption of SAC could significantly reduce the levels of COX-2 positively stained cells in vivo. Quantitative results also showed that SAC could significantly reduce the COX-2 expression level from the results of immunohistochemical staining. These results suggested that the inhibitory effect of SAC on lung carcinoma is associated with the reduced levels of COX-2 proteins in tumor-bearing mice. Taken together, it is probable that SAC could inhibit the malignant progression of lung carcinoma in part through suppression of NF- κ B and COX-2 proteins.

DISCUSSION

SAC, a sulfur-containing amino acid, is generated from a soaking preparation of garlic. The SAC content is around 30 μ g/g of fresh garlic (24). Recent studies indicated that SAC could have

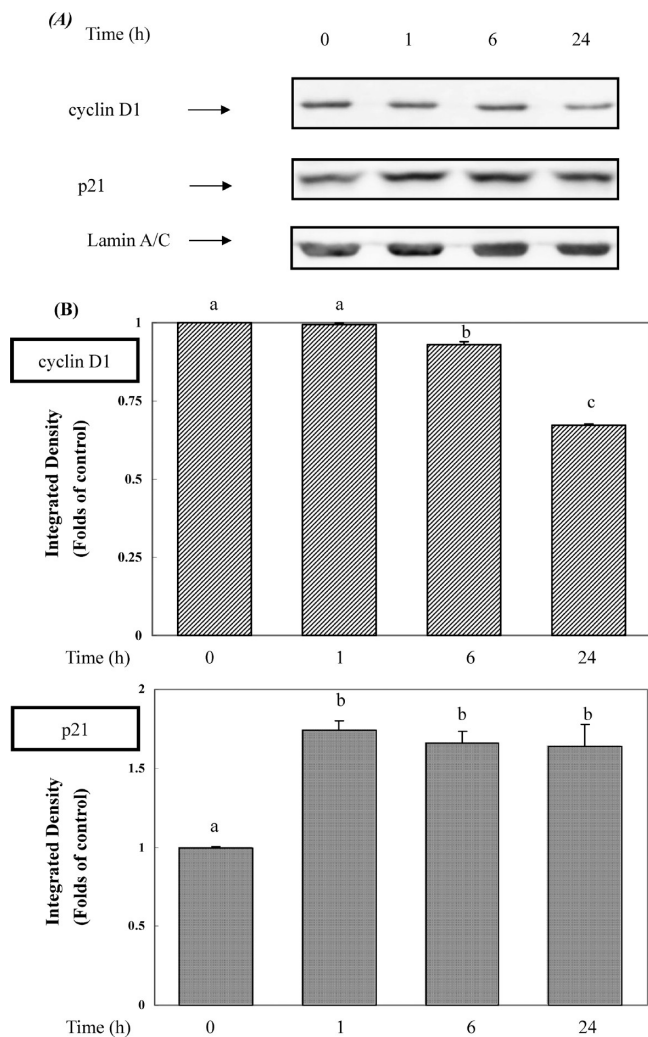


Figure 3. SAC modulated the expression of cyclin D1 proteins in human NSCLC A-549 cells. **(A)** Postconfluent lung cancer cells cultured on 10 cm culture dishes were incubated in RPMI-1640 medium with 10% fetal bovine serum at 37 °C. After washing out the media, lung cancer cells were incubated with SAC (20 mM) for different time points. Cell lysates from A-549 cells were prepared using an NE-PER reagent kit containing protease inhibitor according to the manufacturer's instruction. After centrifugation for 10 min at 12000g to remove cell debris, the supernatants were retained as a cytoplasmic extract. Cross-contamination between nuclear and cytoplasmic fractions were not found (data not shown). Nuclear lysates were blotted with anti-cyclin D1 and anti-p21 monoclonal antibodies as described under Materials and Methods. The levels of detection in cell lysate represent the amount of cyclin D1 and p21 proteins in human lung cancer cells. The blots were stripped and reprobed with anti-lamin A/C antibody as loading control. The results presented are representative of three different experiments. The immunoreactive bands are noted with arrows. **(B)** The integrated density of cyclin D1 and p21 proteins adjusted with internal control protein (lamin A/C) are shown. Different letters represent statistically significant difference, $p < 0.05$.

antioxidant activity (25, 26), cancer chemoprevention effect (27), and antihepatopathic activity (28). Our previous study also indicated that SAC could suppress the proliferation and malignant progression of human oral cancer cells through the modulation of cellular signaling pathways (29). The phosphoinositide 3-kinase (PI3K)/Akt/mTOR signaling pathways have been shown to be the predominant growth-factor-activated pathways and play important roles in the proliferation and survival of NSCLC (30, 31). Activated Akt/mTOR signaling pathways have

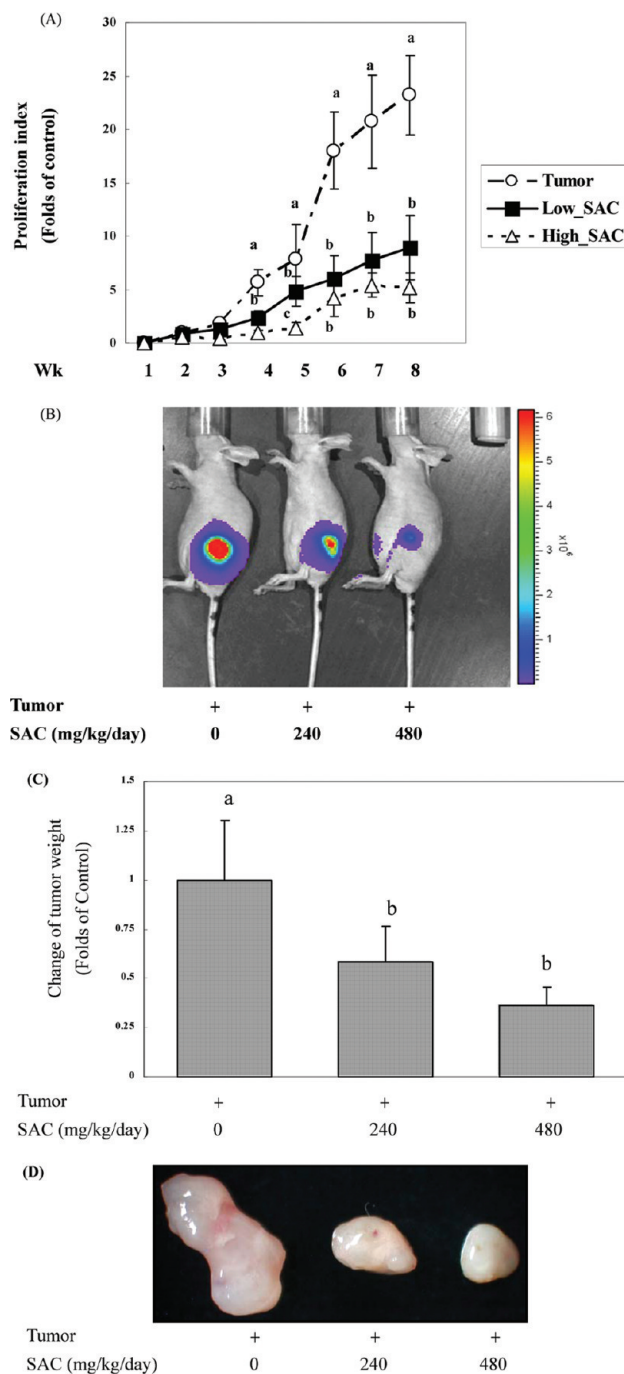


Figure 4. Consumption of SAC suppressed the growth of lung carcinoma in vivo. **(A)** Xenograft nude mice ($n = 6$ for each group) were divided into three groups (tumor, tumor with low SAC, tumor with high SAC) and given SAC (0, 240, and 480 mg/kg of body weight/day) for 8 weeks. The extent of tumor growth was evaluated by using a bioluminescent imaging system. Data of bioluminescent intensity represent the proliferation index in primary tumor tissues. Different letters represent statistically significant difference, $p < 0.05$. **(B)** Xenograft nude mice were given SAC (240 and 480 mg/kg of body weight/day) for 8 weeks. The extent of tumor growth was evaluated by using bioluminescent imaging system. Data represent the bioluminescent intensity of primary tumor tissues at week 8. **(C)** Data represent the change of tumor weight among control, 240 mg/kg/day SAC, and 480 mg/kg/day SAC groups. Different letters represent statistically significant difference, $p < 0.05$ ($p < 0.05$ at week 8). **(D)** Human NSCLC A-549 cell implanted nude mice were given SAC (0, 240, and 480 mg/kg of body weight/day) for 8 weeks. Photos of primary tumors from different groups are shown.

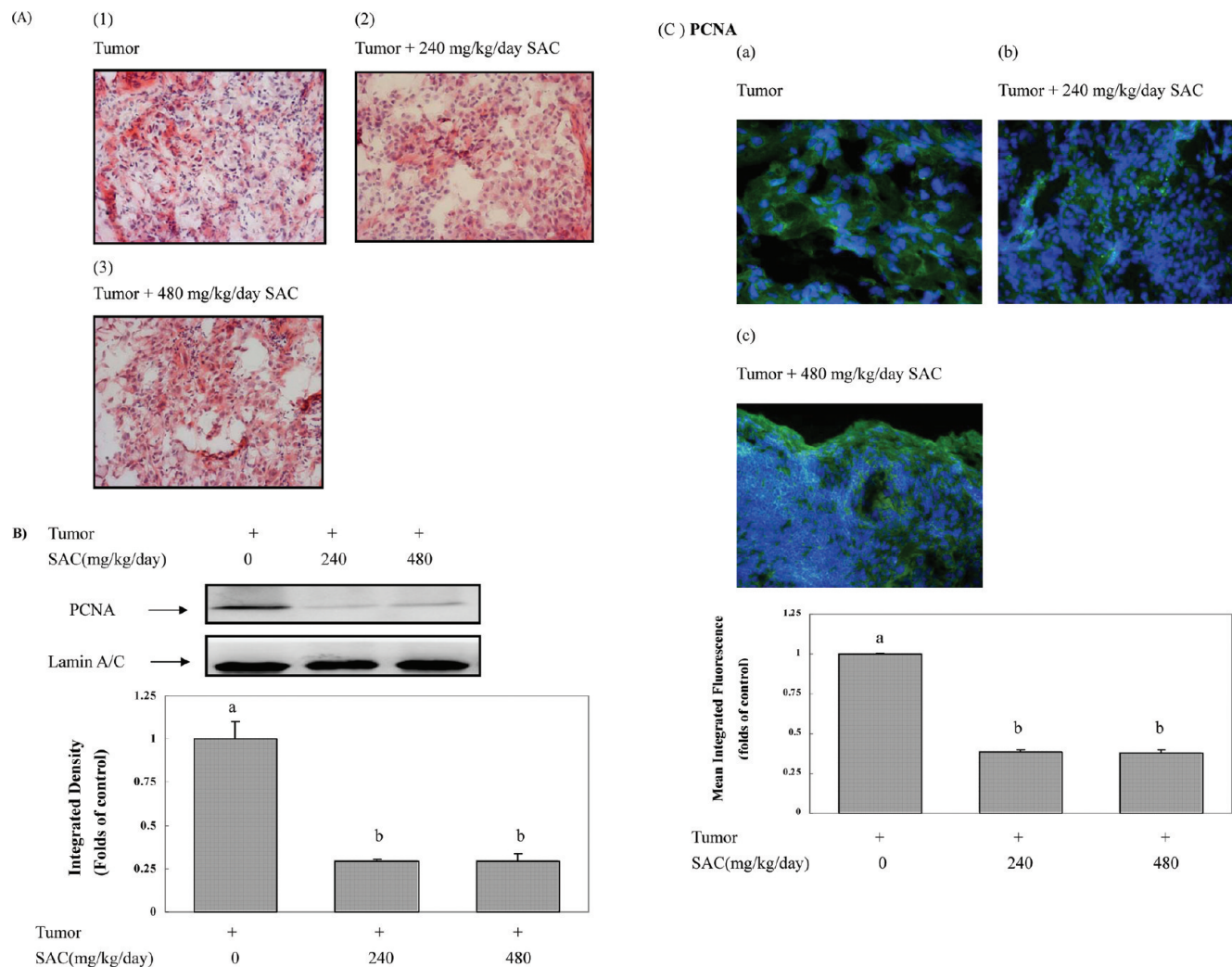


Figure 5. Inhibitory effects of SAC on cellular proliferation are associated with the reduced expression of PCNA protein in NSCLC A-549 cell transplanted nude mice. **(A)** Normal tissue and primary lung cancer tissue were formalin-fixed, embedded in paraffin, sectioned, and subjected to H&E staining. Imaging was documented at $200\times$ magnification. Blue spots represent the nuclei stained with hematoxylin. Red spots represent cytoplasm stained with eosin. **(B)** Cell lysates from animal tissues were prepared using a Tissue Extract reagent kit containing protease inhibitor and phosphatase inhibitors according to the manufacturer's instruction. After centrifugation for 10 min at $12000g$ to remove cell debris, the supernatants were retained as a whole tissue extract. Cross-contamination between nuclear and cytoplasm fractions were not found (data not shown). Cell lysates were blotted with anti-PCNA monoclonal antibody as described under Materials and Methods. The levels of detection in cell lysate represent the amount of PCNA in human lung cancer cells. The blots were stripped and reprobed with anti-lamin A/C antibody as loading control. The results presented are representative of three different experiments. The immunoreactive bands are noted with arrows. The integrated density of PCNA protein adjusted with internal control protein (lamin A/C) is shown in the bottom panel. Different letters represent statistically significant difference, $p < 0.05$. **(C)** Normal tissue and primary lung cancer tissue were frozen, sectioned, and subjected to anti-PCNA antibody by immunohistochemical staining described under Materials and Methods. Imaging was documented at $200\times$ magnification. Green fluorescence area represents distribution of PCNA protein in A-549 cells stained with monoclonal antibody. Blue fluorescence area represents the location of cell nuclei stained with 4,6-diamidino-2-phenylindole (DAPI). The results presented are representative of six different experiments. The mean integrated fluorescence of PCNA protein is shown in the bottom panel. Different letters represent statistically significant difference, $p < 0.05$.

been observed in NSCLC and uncovered essential roles in the control of gene expression and protein translation, which affect cellular proliferation and tumor angiogenesis. Previous studies indicated PI3K-dependent phosphorylation of Akt or mTOR molecules in a panel of NSCLC cell lines, which was correlated with resistance to chemotherapy (3). The mTOR inhibitor rapamycin alone or in combination with chemotherapy treatment rendered NSCLC cell lines with high Akt/mTOR more responsive to apoptosis and growth inhibition (7, 12). Collectively, these pieces of evidence show significant roles of the activated EGFR and PI3K/Akt/mTOR pathway in NSCLC. Our results demonstrated that activation of PI3K/Akt and NF- κ B signaling

pathways plays important roles in the cell proliferation of human NSCLC A-549 cells in vitro (Figure 2A). Previous studies suggested that phytochemicals in fruits and vegetables might have anticancer effects (32–34). *Allium* vegetables, especially garlic, has been implicated as anticancer agents in many studies (35–37). Previous studies showed that SAC could inhibit the proliferation of several types of cancer including prostate and breast cancers (27, 38). SAC at different concentrations (2.5–40 mM) could significantly inhibit the proliferation of breast cancer cells between one and seven days (27). These results suggested that SAC might effectively suppress the growth of human cancer cells at a long-term period. Our previous study also demonstrated the

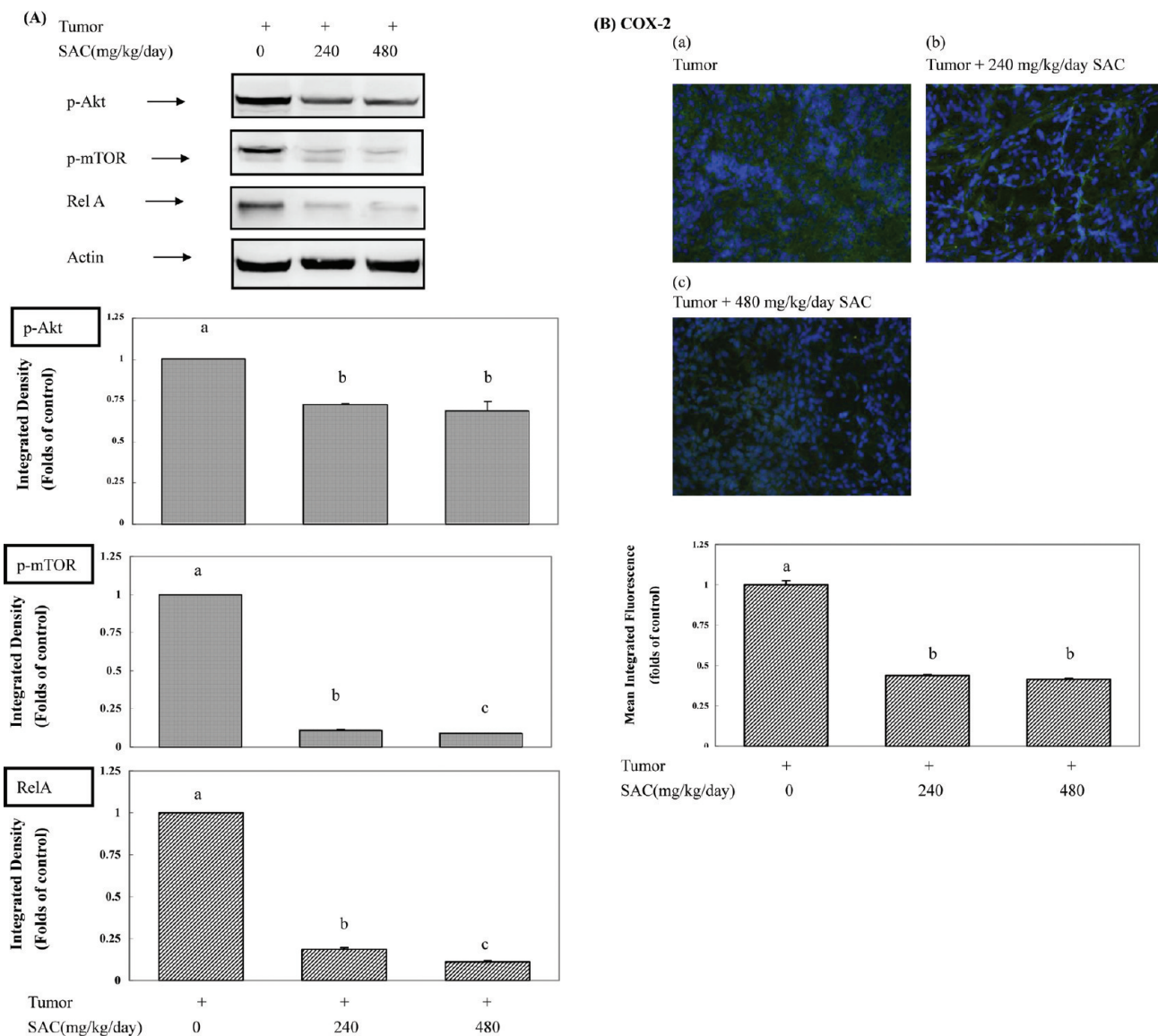


Figure 6. Consumption of SAC suppressed the malignant progression of lung carcinoma and modulated the expression of NF- κ B and COX-2 proteins in tumor-bearing mice. **(A)** Cell lysates from animal tissues were prepared using a Tissue Extract reagent kit containing protease inhibitor and phosphatase inhibitors according to the manufacturer's instruction. After centrifugation for 10 min at 12000g to remove cell debris, the supernatants were retained as a whole tissue extract. Cross-contamination between nuclear and cytoplasmic fractions was not found (data not shown). Cell lysates were blotted with antiphosphorylation Akt, antiphosphorylation mTOR, and anti-NF- κ B p65 (Rel A) monoclonal antibodies as described under Materials and Methods. The levels of detection in cell lysate represent the amount of phosphorylated Akt, phosphorylated mTOR, and NF- κ B in human lung cancer cells. The blots were stripped and reprobed with anti-actin antibody as loading control. The results presented are representative of three different experiments. The immunoreactive bands are noted with arrows. The integrated densities of p-Akt, p-mTOR, and Rel A proteins adjusted with internal control protein (actin) are shown in the panel. Different letters represent statistically significant difference, $p < 0.05$. **(B)** Normal tissue and primary lung cancer tissue were frozen, sectioned, and subjected to anti-COX-2 antibody by immunohistochemical staining described under Materials and Methods. Imaging was documented at 200 \times magnification. Green fluorescence area represents distribution of COX-2 protein in A-549 cells stained with monoclonal antibody. Blue fluorescence area represents the location of cell nuclei stained with 4,6-diamidino-2-phenylindole (DAPI). The results presented are representative of six different experiments. The mean integrated fluorescence of COX-2 protein is shown in the bottom panel. Different letters represent statistically significant difference, $p < 0.05$.

inhibitory effects of SAC on the growth of human oral cancer cells in vitro (29). In the current study, we examined whether SAC could inhibit the proliferation of highly invasive human NSCLC A-549 cells in vitro. To investigate the molecular mechanisms of actions, we used high concentrations of SAC (5–20 mM) in the in vitro cell model. At 24 h, SAC (at concentrations of 5, 10, and 20 mM) inhibited the proliferation of NSCLC A-549 cells up to 10, 17, and 30%, respectively (Figure 1A). Furthermore, SAC could significantly suppress cell proliferation at 72 h by up to 37, 59, and 71%, respectively (Figure 1). SAC at different concentrations (5–20 mM) could effectively inhibit the proliferation of human

NSCLC A-549 cells. The concentration of SAC used in the present experiment was similar with the one in other studies (27). Our results were consistent with our previous findings and indicated that SAC could act as a chemopreventive agent against human NSCLC A-549 cancer cells. We concluded that the effective concentration of SAC is relatively high in several studies; perhaps it is a water-soluble organosulfur compound from garlic. We further demonstrated that SAC could significantly inhibit the action of mTOR and NF- κ B p65 (Rel A) proteins in human NSCLC A-549 cells in a time-dependent manner (Figure 2B,C). Our results also demonstrated that SAC could modulate cell-cycle

inhibitor p21^{CIP1/WAF1} and suppress the expression of cyclin D1 (Figure 3). To distinguish whether the inhibitory effects of SAC were through the general reducing effects of SH⁻ reagents, we also examined and compared the effects of reduced glutathione on the proliferation of human NSCLC A-549 cells in vitro. Our results did not show significant effects of reduced glutathione on the suppression of A-549 cancer cells in comparison to SAC (data not shown). Therefore, the anticancer effects of SAC observed in this study are specifically targeting human NSCLC A-549 cancer cells. These results also suggest that SAC could modulate the cell signaling pathways in human NSCLC A-549 cancer cells, although the detailed mechanisms of SAC/cancer cell interaction are still under investigation.

To further investigate the inhibitory effects of SAC in vivo, we adapted a mouse xenograft model by inoculating human NSCLC A-549 cells into nude mice. Previous study did not show any toxicity effects while experimental mice received daily consumption of SAC at 250–2000 mg/kg (24). Therefore, we used moderately high levels of SAC (240 and 480 mg/kg) to examine the in vivo chemoprevention effect. No differences in food intake or body weight were observed in the present study (data not shown). As shown in Figure 4, our study indicated that consumption of SAC at 240 mg/kg of BW (low dosage) and 480 mg/kg of BW (high dosage) could significantly inhibit the growth of NSCLC A-549 cell bearing nude mice without any apparent untoward toxicity (data not shown). To confirm our findings, we further demonstrated the inhibitory effects of SAC on the growth of lung carcinoma by using the in vivo bioluminescence imaging system. Bioluminescence imaging results indicated that SAC significantly blocked tumor growth in the mouse xenograft model. Pathological staining results indicated that SAC could effectively block the proliferation and malignant progression of human NSCLC A-549 cells in nude mice (Figure 5A). The present study showed that SAC could also inhibit the tumor growth and levels of PCNA positively stained cells in tumor tissues (Figure 5C). These pieces of evidence proved the chemopreventive effects of SAC against highly malignant lung carcinoma.

It is well-known that proliferation, angiogenesis, and malignant progression of lung cancer are correlated with the overexpression of COX-2 protein. It is already known that NF- κ B transcription factor plays an important role in the modulation of COX-2 expression. To examine whether SAC could block the malignant progression of human NSCLC A-549 cells, we investigated the effects of SAC on the levels of COX-2 positively stained cells. Our results showed that SAC could significantly reduce levels of COX-2 positively stained cells in tumor-bearing mice (Figure 6B). In this study, we also demonstrated that the PI3K/Akt and NF- κ B signaling pathways played important roles in the regulation of cellular proliferation. Furthermore, our results showed that SAC could effectively inhibit the activation of Akt/mTOR signaling pathways. SAC could also significantly inhibit the nuclear activation of NF- κ B molecules. Take together, these results indicated that SAC could effectively inhibit the proliferation and malignancy of lung cancer in tumor-bearing mice.

In conclusion, our results demonstrate a novel finding that daily consumption of SAC at a concentration of 240 or 480 mg/kg of BW/day could suppress the growth and malignant progression of lung carcinoma in a mouse xenograft model. SAC could inhibit the activation of Akt/mTOR signaling pathways, NF- κ B molecule, and the expression of COX-2 protein in tumor-bearing mice. In the present study, we demonstrated the anticancer effects of SAC on the growth of human NSCLC A-549 cancer cells in vivo. Furthermore, we are also aware of the physiological relevance of SAC for the future study. Currently, we are investigating the chemopreventive effects of SAC on different types of human

cancer cells even at low dosages (≤ 60 mg/kg). Take together, these results still provide important evidence and suggest that SAC might be an effective chemopreventive agent against highly invasive lung carcinoma.

LITERATURE CITED

- (1) Molina, J. R.; Yang, P.; Cassivi, S. D.; Schild, S. E.; Adjei, A. A. Non-small cell lung cancer: epidemiology, risk factors, treatment, and survivorship. *Mayo Clin. Proc.* **2008**, *83*, 584–594.
- (2) Sher, T.; Dy, G. K.; Adjei, A. A. Small cell lung cancer. *Mayo Clin. Proc.* **2008**, *83*, 355–367.
- (3) Brognard, J.; Clark, A. S.; Ni, Y.; Dennis, P. A. Akt/protein kinase B is constitutively active in non-small cell lung cancer cells and promotes cellular survival and resistance to chemotherapy and radiation. *Cancer Res.* **2001**, *61*, 3986–3997.
- (4) Vogt, P. K.; Kang, S.; Elsliger, M. A.; Gymnopoulos, M. Cancer-specific mutations in phosphatidylinositol 3-kinase. *Trends Biochem. Sci.* **2007**, *32*, 342–349.
- (5) Aoki, M.; Blazek, E.; Vogt, P. K. A role of the kinase mTOR in cellular transformation induced by the oncoproteins P3k and Akt. *Proc. Natl. Acad. Sci. U.S.A.* **2001**, *98*, 136–141.
- (6) Morgensztern, D.; McLeod, H. L. PI3K/Akt/mTOR pathway as a target for cancer therapy. *Anticancer Drugs* **2005**, *16*, 797–803.
- (7) Zou, Z. Q.; Zhang, X. H.; Wang, F.; Shen, Q. J.; Xu, J.; Zhang, L. N.; Xing, W. H.; Zhuo, R. J.; Li, D. A novel dual PI3K α /mTOR inhibitor PI-103 with high antitumor activity in non-small cell lung cancer cells. *Int. J. Mol. Med.* **2009**, *24*, 97–101.
- (8) Gao, N.; Flynn, D. C.; Zhang, Z.; Zhong, X. S.; Walker, V.; Liu, K. J.; Shi, X.; Jiang, B. H. G1 cell cycle progression and the expression of G1 cyclins are regulated by PI3K/AKT/mTOR/p70S6K1 signaling in human ovarian cancer cells. *Am. J. Physiol. Cell Physiol.* **2004**, *287*, C281–C291.
- (9) Gao, N.; Zhang, Z.; Jiang, B. H.; Shi, X. Role of PI3K/AKT/mTOR signaling in the cell cycle progression of human prostate cancer. *Biochem. Biophys. Res. Commun.* **2003**, *310*, 1124–1132.
- (10) Cayrol, C.; Ducommun, B. Interaction with cyclin-dependent kinases and PCNA modulates proteasome-dependent degradation of p21. *Oncogene* **1998**, *17*, 2437–2444.
- (11) Cayrol, C.; Knibiehler, M.; Ducommun, B. p21 binding to PCNA causes G1 and G2 cell cycle arrest in p53-deficient cells. *Oncogene* **1998**, *16*, 311–320.
- (12) Pal, S. K.; Figlin, R. A.; Reckamp, K. L. The role of targeting mammalian target of rapamycin in lung cancer. *Clin. Lung Cancer* **2008**, *9*, 340–345.
- (13) Gadgil, S. M.; Ali, S.; Philip, P. A.; Ahmed, F.; Wozniak, A.; Sarkar, F. H. Response to dual blockade of epidermal growth factor receptor (EGFR) and cyclooxygenase-2 in nonsmall cell lung cancer may be dependent on the EGFR mutational status of the tumor. *Cancer* **2007**, *110*, 2775–2784.
- (14) Chun, K. S.; Surh, Y. J. Signal transduction pathways regulating cyclooxygenase-2 expression: potential molecular targets for chemoprevention. *Biochem. Pharmacol.* **2004**, *68*, 1089–1100.
- (15) Gadgil, S. M.; Ali, S.; Philip, P. A.; Wozniak, A.; Sarkar, F. H. Genistein enhances the effect of epidermal growth factor receptor tyrosine kinase inhibitors and inhibits nuclear factor kappa B in nonsmall cell lung cancer cell lines. *Cancer* **2009**, *115*, 2165–2176.
- (16) Peng, G.; Dixon, D. A.; Muga, S. J.; Smith, T. J.; Wargovich, M. J. Green tea polyphenol (–)-epigallocatechin-3-gallate inhibits cyclooxygenase-2 expression in colon carcinogenesis. *Mol. Carcinog.* **2006**, *45*, 309–319.
- (17) Hong, Y. S.; Ham, Y. A.; Choi, J. H.; Kim, J. Effects of allyl sulfur compounds and garlic extract on the expression of Bcl-2, Bax, and p53 in non small cell lung cancer cell lines. *Exp. Mol. Med.* **2000**, *32*, 127–134.
- (18) Srivastava, S. K.; Hu, X.; Xia, H.; Zaren, H. A.; Chatterjee, M. L.; Agarwal, R.; Singh, S. V. Mechanism of differential efficacy of garlic organosulfides in preventing benzo(a)pyrene-induced cancer in mice. *Cancer Lett.* **1997**, *118*, 61–67.
- (19) Knowles, L. M.; Milner, J. A. Allyl sulfides modify cell growth. *Drug Metab. Drug Interact.* **2000**, *17*, 81–107.

- (20) Knowles, L. M.; Milner, J. A. Possible mechanism by which allyl sulfides suppress neoplastic cell proliferation. *J. Nutr.* **2001**, *131*, 1061S–1066S.
- (21) Sakamoto, K.; Lawson, L. D.; Milner, J. A. Allyl sulfides from garlic suppress the in vitro proliferation of human A549 lung tumor cells. *Nutr. Cancer* **1997**, *29*, 152–156.
- (22) Fleischauer, A. T.; Poole, C.; Arab, L. Garlic consumption and cancer prevention: meta-analyses of colorectal and stomach cancers. *Am. J. Clin. Nutr.* **2000**, *72*, 1047–1052.
- (23) Fleischauer, A. T.; Arab, L. Garlic and cancer: a critical review of the epidemiologic literature. *J. Nutr.* **2001**, *131*, 1032S–1040S.
- (24) Kodera, Y.; Suzuki, A.; Imada, O.; Kasuga, S.; Sumioka, I.; Kanezawa, A.; Taru, N.; Fujikawa, M.; Nagae, S.; Masamoto, K.; Maeshige, K.; Ono, K. Physical, chemical, and biological properties of *S*-allylcysteine, an amino acid derived from garlic. *J. Agric. Food Chem.* **2002**, *50*, 622–632.
- (25) Elinos-Calderon, D.; Robledo-Arratia, Y.; Perez-De La Cruz, V.; Maldonado, P. D.; Galvan-Arzate, S.; Pedraza-Chaverri, J.; Santamaria, A. Antioxidant strategy to rescue synaptosomes from oxidative damage and energy failure in neurotoxic models in rats: protective role of *S*-allylcysteine. *J. Neural Transm.* **2010**, *117*, 35–44.
- (26) Garcia, E.; Villeda-Hernandez, J.; Pedraza-Chaverri, J.; Maldonado, P. D.; Santamaria, A. *S*-Allylcysteine reduces the MPTP-induced striatal cell damage via inhibition of pro-inflammatory cytokine tumor necrosis factor- α and inducible nitric oxide synthase expressions in mice. *Phytomedicine* **2010**.
- (27) Gapter, L. A.; Yuin, O. Z.; Ng, K. Y. *S*-Allylcysteine reduces breast tumor cell adhesion and invasion. *Biochem. Biophys. Res. Commun.* **2008**, *367*, 446–451.
- (28) Shinkawa, H.; Takemura, S.; Minamiyama, Y.; Kodai, S.; Tsukioka, T.; Osada-Oka, M.; Kubo, S.; Okada, S.; Suehiro, S. *S*-Allylcysteine is effective as a chemopreventive agent against porcine serum-induced hepatic fibrosis in rats. *Osaka City Med. J.* **2009**, *55*, 61–69.
- (29) Tang, F. Y.; Chiang, E. P.; Chung, J. G.; Lee, H. Z.; Hsu, C. Y. *S*-Allylcysteine modulates the expression of E-cadherin and inhibits the malignant progression of human oral cancer. *J. Nutr. Biochem.* **2009**, *20*, 1013–1020.
- (30) Boehle, A. S.; Kurdow, R.; Boenicke, L.; Schniewind, B.; Faendrich, F.; Dohrmann, P.; Kalthoff, H. Wortmannin inhibits growth of human non-small-cell lung cancer in vitro and in vivo. *Langenbecks Arch. Surg.* **2002**, *387*, 234–239.
- (31) Liao, D. W.; Wang, L.; Zhang, X. G.; Liu, M. Q. [Expression and significance of PTEN/PI3K signal transduction-related proteins in non-small cell lung cancer]. *Ai Zheng* **2006**, *25*, 1238–1242.
- (32) Amin, A. R.; Kucuk, O.; Khuri, F. R.; Shin, D. M. Perspectives for cancer prevention with natural compounds. *J. Clin. Oncol.* **2009**, *27*, 2712–2725.
- (33) Lampe, J. W. Interindividual differences in response to plant-based diets: implications for cancer risk. *Am. J. Clin. Nutr.* **2009**, *89*, 1553S–1557S.
- (34) Beliveau, R.; Gingras, D. Role of nutrition in preventing cancer. *Can. Fam. Physician* **2007**, *53*, 1905–1911.
- (35) Singh, S. V.; Powolny, A. A.; Stan, S. D.; Xiao, D.; Arlotti, J. A.; Warin, R.; Hahm, E. R.; Marynowski, S. W.; Bommareddy, A.; Potter, D. M.; Dhir, R. Garlic constituent diallyl trisulfide prevents development of poorly differentiated prostate cancer and pulmonary metastasis multiplicity in TRAMP mice. *Cancer Res.* **2008**, *68*, 9503–9511.
- (36) Galeone, C.; Pelucchi, C.; Dal Maso, L.; Negri, E.; Montella, M.; Zucchetto, A.; Talamini, R.; La Vecchia, C. *Allium* vegetables intake and endometrial cancer risk. *Public Health Nutr.* **2009**, *12*, 1576–1579.
- (37) Powolny, A. A.; Singh, S. V. Multitargeted prevention and therapy of cancer by diallyl trisulfide and related *Allium* vegetable-derived organosulfur compounds. *Cancer Lett.* **2008**, *269*, 305–314.
- (38) Chu, Q.; Lee, D. T.; Tsao, S. W.; Wang, X.; Wong, Y. C. *S*-Allylcysteine, a water-soluble garlic derivative, suppresses the growth of a human androgen-independent prostate cancer xenograft, CWR22R, under in vivo conditions. *BJU Int.* **2007**, *99*, 925–932.

Received for review July 2, 2010. Revised manuscript received August 28, 2010. Accepted August 30, 2010. This material is based upon work supported, in part, by a National Science Council grant, under agreement 97-2320-B-039-043-MY3, NSC97-2321-B-005-005, and by a China Medical University (CMU) grant under agreement CMU97-129 and CMU97-186. Any opinions, findings, conclusions, or recommendations expressed in this publication are those of the author(s) and do not necessarily reflect the view of the National Science Council and China Medical University.